

# <sup>13</sup>C and <sup>15</sup>N CP/MAS NMR Characterization of MDI-Polyisocyanurate Resin Systems

David W. Duff and Gary E. Maciel\*

Department of Chemistry, Colorado State University, Fort Collins, Colorado 80523

Received March 22, 1989; Revised Manuscript Received November 28, 1989

**ABSTRACT:** A series of MDI-polyisocyanurate resins were prepared under a variety of reaction conditions from 4,4'-methylenebis(phenylisocyanate) (MDI) and from <sup>15</sup>N-enriched MDI, using stannous octoate as catalyst. The formation of cross-links via isocyanurate ring formation and the fate of the unreacted isocyanate were monitored by both <sup>13</sup>C and <sup>15</sup>N CP/MAS NMR methods, and an optimal cure temperature of ca. 120 °C was determined for this particular system. Urea linkages and other less predominant structures such as amine, biuret, and uretidione were clearly identified by <sup>15</sup>N CP/MAS. The ability of <sup>15</sup>N CP/MAS to yield quantitative results on the extent of cross-linking is demonstrated. <sup>15</sup>N CP/MAS proves to be a powerful technique for structure elucidation in these complex macromolecular systems.

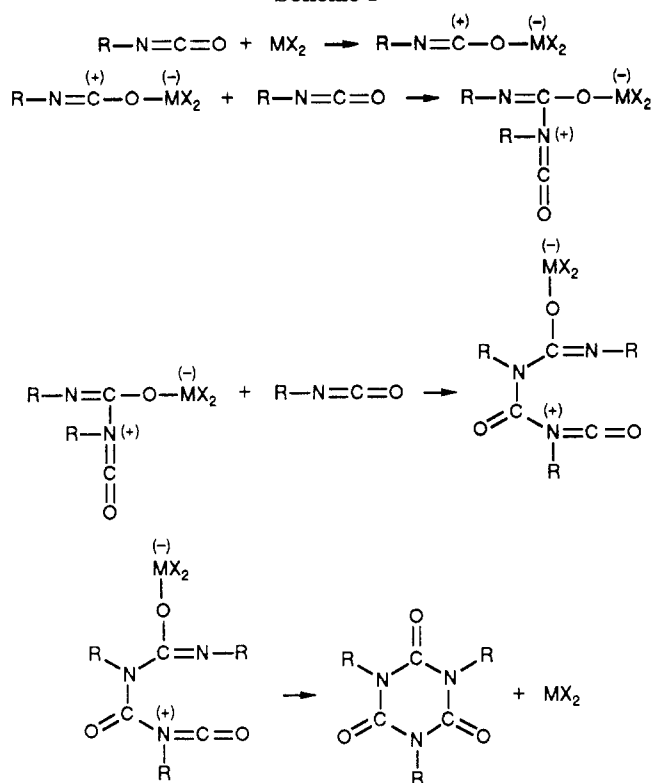
## Introduction

4,4'-Methylenebis(phenyl isocyanate) (MDI) is a difunctional monomer with widespread use in the foam, adhesive, construction, and related industries.<sup>1-3</sup> Because of the reactivity of the isocyanate functional group, systems based on MDI are amenable to many potential chemical modifications, resulting in a wide variety of physical, mechanical and/or chemical characteristics. The modification of polyurethanes with isocyanurate cross-links to produce materials with enhanced thermal and dimensional stabilities has been known for some time<sup>4-6</sup> and continues to be an active area of investigation.<sup>7-12</sup> This paper addresses the study of the isocyanurate linkage directly by examining MDI-based resin systems tailored with a high density of isocyanurate cross-links. Characterization of the isocyanurate linkages and elucidation of the curing behavior leading to their formation should prove to be a useful foundation for future investigations of systems containing such linkages. The NMR results presented here emphasize chemical structural patterns, trends, and relationships and are not meant to correlate directly with physical properties or commercial products. Indeed, the resin systems prepared for this study bear little resemblance to commercial products of which we are aware and were prepared for the purpose of making possible the exploration of a diverse array of chemical structures in relation to NMR measurements. It is hoped that this study will be helpful in designing experiments aimed more directly at materials with technologically useful physical/mechanical properties.

Solid-state CP/MAS NMR<sup>13-15</sup> is ideally suited for studying cured resins,<sup>16-20</sup> such as those of this study, with limited solubility. Dissolution of such materials might remove the fundamental physical, mechanical, and/or chemical properties associated with the important characteristics of the solid matrix. Since it is these types of properties that are often of primary interest in these materials, the use of a nondestructive solid-state technique like CP/MAS NMR is indicated. Very little NMR characterization of isocyanurate-based systems has been carried out,<sup>21</sup> and no solid-state investigations have been reported.

The Lewis acid catalyzed polymerization of isocyanates allows for the formation of several products.<sup>22-24</sup> In the initiation step,<sup>24</sup> a suitable Lewis acid, such as

Scheme I

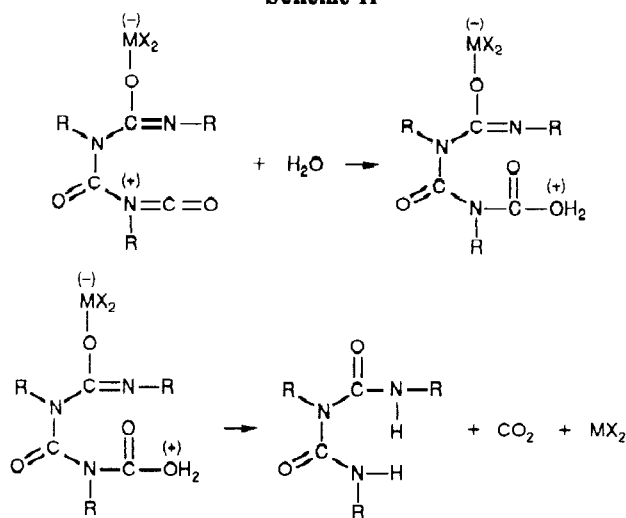


stannous octoate ( $MX_2$ ), attacks the isocyanate group, generating a metal-ether complex containing an activated carbon center. Nucleophilic attack of isocyanate on this activated center generates another activated site (carbonyl) for further nucleophilic attack by more isocyanate. Finally, expulsion of catalyst results in ring closure, yielding the isocyanurate cross-link (Scheme I). In addition to formation of isocyanurate linkages, formation of biuret linkages can also occur (Scheme II). In this case, water acts as a nucleophile, attacking the activated carbonyl of an isocyanate. Loss of  $CO_2$  and catalyst yields the biuret, which characteristically contains amide and imide nitrogens. Since MDI is a difunctional monomer, branching can occur from any available isocyanate, leading to a highly cross-linked, insoluble resin.

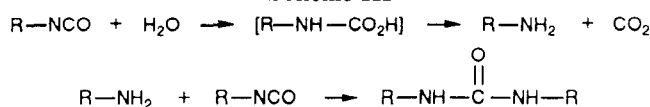
In addition to the catalytic pathways outlined in Schemes I and II, unreacted isocyanate functionalities

\* To whom correspondence should be addressed.

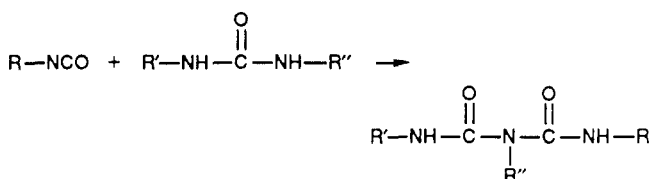
Scheme II



Scheme III



Scheme IV



can react in the absence of catalyst with compounds that contain active hydrogens. Hence, samples that are left unprotected from air after the initial cure period should readily react with water vapor, producing urea linkages. A free isocyanate reacts with water to form a carbamic acid, which loses  $CO_2$  to form the free amine. The amine, once formed, quickly reacts with the excess isocyanate to form a urea structure<sup>22</sup> (Scheme III). Isocyanate can then react with urea linkages via their active hydrogen atoms, resulting in the formation of biuret linkages<sup>22</sup> (Scheme IV).

The various types of chemistry outlined in these reaction schemes are conveniently amenable individually to investigation by specific solid-state NMR techniques. Identifying pertinent chemical structures by solid-state NMR and determining the conditions that favor isocyanurate ring formation and the extents of the various competing species are the focus of this paper.

### Experimental Section

**NMR Measurements.**  $^{13}C$  CP/MAS spectra were obtained at 50.3 MHz on a modified wide-bore Nicolet NT-200 spectrometer. The  $^{13}C$  NMR parameters used to accumulate the spectra shown in this paper were, unless otherwise indicated, a 4-ms contact time and a 6-s repetition time. Samples were spun at 6.5 kHz, using Chemagnetics' zirconia bullet spinners;<sup>25</sup> the magic angle was adjusted to within  $0.1^\circ$  by using the  $^{79}Br$  spectrum of KBr placed in a spinner.<sup>26</sup>

$^{15}N$  CP/MAS spectra were obtained at 20.3 MHz on the same modified NT-200 spectrometer. The NMR parameters used to accumulate the spectra shown here were, unless otherwise indicated, a 6-ms contact time and a 6-s repetition time. MDI-

based polymeric samples were spun at 3.0 kHz, using bullet-type spinners, and the magic angle was again set by using the KBr method. Model compounds for  $^{15}N$  natural-abundance measurements were studied at a MAS speed of 3.0 kHz, using a large-volume MAS assembly;<sup>27</sup> the magic angle was set by using the KBr method. Pertinent experimental conditions for obtaining the spectra of the model compounds are given in Table I.

Proton-decoupled liquid-solution  $^{13}C$  and  $^{15}N$  spectra were obtained on a Bruker AM-500 spectrometer at a carbon frequency of 125.8 MHz and a nitrogen frequency of 50.7 MHz. All  $^{13}C$  spectra were referenced externally to tetramethylsilane at 0 ppm and all  $^{15}N$  spectra to liquid  $NH_3$ , also at 0 ppm.

**Samples.** 4,4'-Methylenebis(phenyl isocyanate) (MDI) was obtained from Eastman Kodak Co. and was purified by distillation through a Vigreux column at reduced pressure (142–145  $^\circ C$  at 0.15 Torr).  $^{15}N$ -Enriched MDI (99.8% doubly labeled) was obtained from MSD Isotopes and was used without further purification to prevent loss of starting material. This possible difference in the integrities of the unlabeled and labeled MDI samples may be responsible for small differences in chemical behaviors noted in the next section. The catalyst, stannous octoate, was obtained from Sigma Chemical Co. and used without further purification. MDI-polyisocyanurate resins were prepared by adding 0.5% catalyst (by weight) to the diisocyanate and heating under a nitrogen atmosphere with stirring at various temperatures for various lengths of time.

### Results and Discussion

Certain peaks in the  $^{13}C$  and  $^{15}N$  CP/MAS NMR spectra obtained in this study were assigned on the basis of comparisons with liquid-solution NMR data from the literature. When no liquid-state data were available in the literature, model compounds were synthesized and examined by  $^{13}C$  and  $^{15}N$  solution-state and, in some cases, solid-state NMR methods. Pertinent  $^{13}C$  and  $^{15}N$  chemical shifts and associated structures are summarized in Table I. One can note that, almost without exception, the solid-state and liquid-solution chemical shifts are within ca.  $\pm 1$  ppm of each other for the model compounds examined by both methods.

Shown in Figure 1 is the static-field dependence of the  $^{13}C$  CP/MAS spectra of a MDI-polyisocyanurate resin cured with stannous octoate at 120  $^\circ C$  for 2 h. The broadening influence of the  $^{14}N$  nucleus on  $^{13}C$  resonances of nearby carbons has been well documented.<sup>28–30</sup> The resonances of  $^{13}C$  nuclei that are located near  $^{14}N$  nuclei are broadened by a combination of the  $^{13}C$ - $^{14}N$  dipolar interaction and the  $^{14}N$  quadrupole effect; the combined effect decreases with increasing field strength. The isocyanurate carbonyl resonance at 150 ppm is barely discernible as a shoulder in the 22.6-MHz spectrum in Figure 1. At 37.5 MHz, the resonance is somewhat resolved, with increased resolution obtained at 50.3 and 90.5 MHz. The resolution of the isocyanurate resonance is good at 90.5 MHz, but the spectrum shown in severely complicated by the presence of spinning sidebands (MAS speed = 3.2 kHz). Sideband suppression techniques were not employed because of our desire to avoid intensity distortions and artifacts.<sup>31</sup> Although MAS speeds in excess of 12 kHz, the speed required to remove the spinning sidebands effectively from these  $^{13}C$  spectra at 90.5 MHz, are routinely employed for other purposes in this laboratory, this method also was not employed because of the uncertainties associated with the cross-polarization dynamics at these high spinning frequencies.<sup>32</sup> For these reasons, the  $^{13}C$  solid-state NMR investigations on the MDI-polyisocyanurate systems of this study were carried out at the compromise field of 4.7 T (50.3 MHz for carbon).

The extent of cross-linking in these MDI-polyisocyanurate resin systems might be estimated by comparing

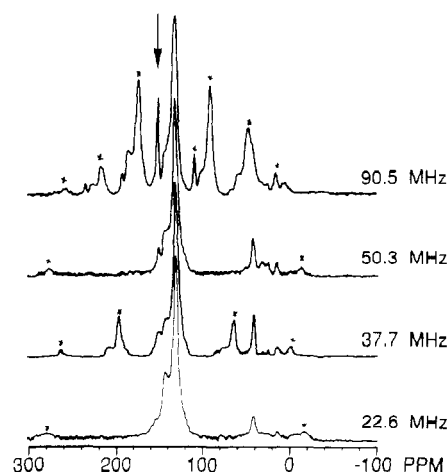


**Figure 1.** Effect of static magnetic field strength on the  $^{13}\text{C}$  CP/MAS spectra (CP contact time =  $\tau$  = 4 ms) of MDI-polyisocyanurate cured with stannous octoate for 2 h at 120  $^{\circ}\text{C}$ . The  $^{13}\text{C}$  Larmor frequency is indicated on the right side of each spectrum. The arrow indicates the position of the isocyanurate carbonyl resonance. Asterisks indicate positions of spinning sidebands.

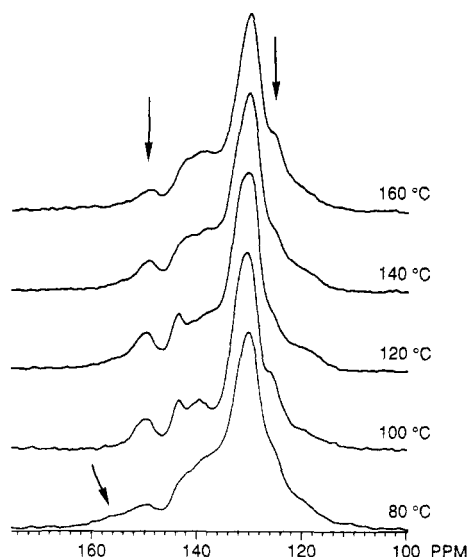


**Figure 2.** 50.3-MHz  $^{13}\text{C}$  CP/MAS spectra ( $\tau$  = 4 ms) of MDI-polyisocyanurate resins prepared at different temperatures. The spectra were expanded to show the pertinent chemical shift range, excluding the methylene carbon resonance at 41 ppm. Arrows indicate specific spectral regions referred to in the text.

the intensities of  $^{13}\text{C}$  CP/MAS resonances due to the isocyanurate ring carbonyl carbons and the unreacted isocyanate carbonyl carbons. In order to establish the usefulness of  $^{13}\text{C}$  and  $^{15}\text{N}$  CP/MAS as potentially quantitative techniques for this kind of purpose, a detailed set of pertinent  $^{13}\text{C}$  and  $^{15}\text{N}$  relaxation experiments was carried out on three  $^{15}\text{N}$ -enriched MDI-polyisocyanurate resins prepared at different cure temperatures. The  $^{15}\text{N}$  results will be discussed in a later section.

Referring to the  $^{13}\text{C}$  chemical shifts in Table I, one sees that the isocyanurate carbons give rise to a resonance centered at ca. 150 ppm, and the region centered about 125 ppm is due to both isocyanate carbonyl carbons and aromatic carbons ortho to an isocyanate functionality.<sup>33</sup> Therefore, the estimation of percent cross-linking based on measuring relative intensities of resonances due to isocyanurate carbonyl carbons and unreacted isocyanate carbonyl resonances by  $^{13}\text{C}$  CP/MAS is not straightforward, since one of the spectral regions of interest contains contributions from at least two types of carbon sites (which may manifest different relaxation behav-

iors). As a result, the  $^{13}\text{C}$  CP/MAS results are discussed here only in a *qualitative* manner, and the quantitative treatment is reserved for the  $^{15}\text{N}$  CP/MAS results.

The 50.3-MHz  $^{13}\text{C}$  CP/MAS spectra of some MDI-polyisocyanurate resins are shown as a function of cure temperature in Figure 2. The spectra have been presented to show the entire chemical shift range relevant to this system, except for the methylene carbon resonance at 41 ppm. The complex spectra shown in Figure 2 are characterized by five resonances or spectral regions arising from the following types of carbon structural situations: a shoulder at 125 ppm due to isocyanate carbonyl carbons and aromatic carbons ortho to an isocyanate functionality; the predominant resonance at 130 ppm due to various hydrogen-bearing aromatic carbons; the region centered about 138 ppm due to benzyl-substituted aromatic carbons para to an isocyanate functionality; the region centered about 143 ppm due to benzyl-substituted aromatic carbons para to an isocyanurate moiety; and a resonance at 150 ppm due to the isocyanurate carbonyl carbons. The following qualitative observations can be made upon inspection of these spectra. First, the shoulder at 125 ppm due to unreacted isocyanate carbonyl carbons and aromatic carbons ortho to isocyanate substituents appears to be most predominant in the spectra of samples prepared at the cure temperatures of 100 and 160  $^{\circ}\text{C}$  (see the arrow on the right in Figure 2) and reaches a minimum relative intensity at a cure temperature of 120  $^{\circ}\text{C}$ . Second, resolution of the benzyl-substituted aromatic carbons para to isocyanurate moieties (143 ppm) is best at the 100 and 120  $^{\circ}\text{C}$  cure temperatures. Third, the isocyanurate carbonyl resonance at 150 ppm appears to have its largest relative intensity at the 100 and 120  $^{\circ}\text{C}$  cure temperatures. From these data, one could tentatively conclude that for these particular reaction conditions, isocyanurate formation is most favored at 100–120  $^{\circ}\text{C}$ . However, the spectra shown in Figure 2 are complex, with isocyanate carbonyl resonances overlapping with the resonances of various aromatic carbons and with other unresolvable resonances that certainly exist in the broad and relatively featureless spectral region between 120 and 145 ppm.

To help identify some of the structures responsible for the 120–145 ppm region, dipolar-dephasing (interrupted decoupling)<sup>34</sup> experiments were carried out on each of the samples represented in Figure 2. In these experiments, a delay period of 70  $\mu\text{s}$  was inserted between the CP contact period and the beginning of data acquisition, during which the  $^1\text{H}$  decoupler is turned off and  $^{13}\text{C}$  magnetization due to  $^{13}\text{C}$ 's that have strong dipolar interactions with protons is attenuated by  $^{13}\text{C}$ – $^1\text{H}$  dipolar dephasing. As a result, the  $^{13}\text{C}$  signal intensity persists for carbons that do not bear hydrogens and methyl carbons (for which  $^{13}\text{C}$ – $^1\text{H}$  dipolar interactions are strongly attenuated by rapid rotation), while signal intensities from methylene and methine carbons are dramatically reduced. However, since the dipolar-dephasing experiment relies on the largely incoherent  $^{13}\text{C}$  spin behavior under  $^{13}\text{C}$ – $^1\text{H}$  and  $^1\text{H}$ – $^1\text{H}$  dipolar interactions, the resulting intensities of the spectrum, especially when overlapping resonances are present, cannot be treated in a quantitative manner. Individual carbons that bear hydrogens can dephase to different extents because of differing strengths of the  $^{13}\text{C}$ – $^1\text{H}$  dipolar interactions and differing rates of  $^1\text{H}$ – $^1\text{H}$  flip flops. Results from these experiments are shown in Figure 3. Clearly, some of the resonances are more clearly resolved than in the "standard spectra" (without dipolar dephasing), with at least five separate resonances clearly

**Table I**  
**Structures and Key NMR Data on Model Compounds<sup>a</sup>**

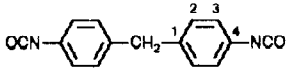
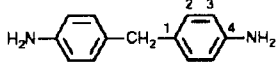
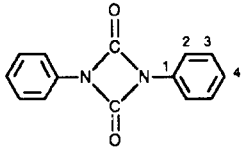
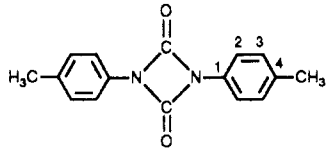
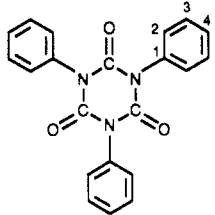
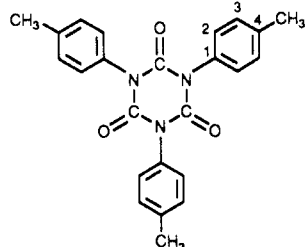
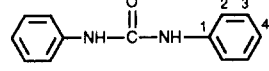
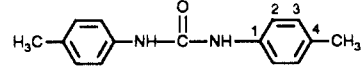
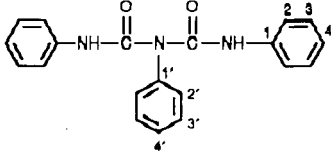
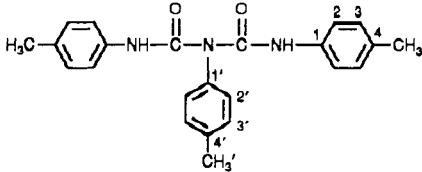
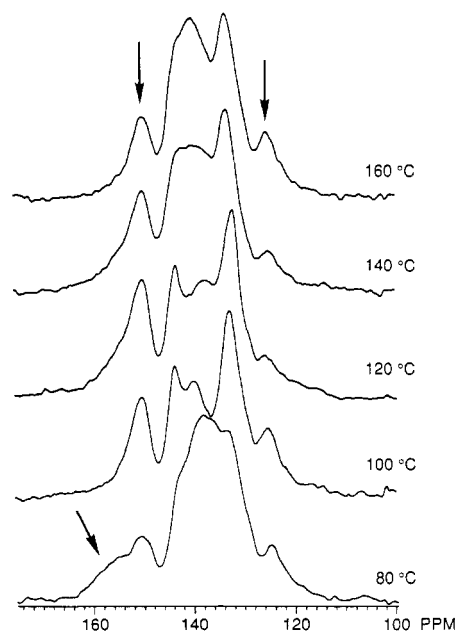
prototype structure	carbon or nitrogen	<sup>13</sup> C chem shift, ppm	<sup>15</sup> N chem shift, ppm	description <sup>b</sup>
 <p align="center">MDI</p>	CH <sub>2</sub> 1 2 3 4 CO N	41 <sup>c</sup> 138 130 (130) <sup>d</sup> 125 (125) 132 125 (125)		methylene carbons methylene-substituted para carbons unsubstituted meta carbons unsubstituted ortho carbons isocyanate-substituted carbons isocyanate carbonyl carbons isocyanate nitrogens
 <p align="center">MDA</p>	CH <sub>2</sub> 1 2 3 4 N	41 <sup>e</sup> 130 129 114 146		methylene carbons methylene-substituted para carbons unsubstituted meta carbons unsubstituted ortho carbons amino-substituted carbons amino nitrogens
 <p align="center">phenyluretidione</p>	1 2 3 4 CO N	135 <sup>i,j</sup> (136) <sup>k</sup> 117 (117) 129 (130) 125 (124) 151 (151)	145 <sup>j</sup>	nitrogen-substituted carbons unsubstituted ortho carbons unsubstituted meta carbons unsubstituted para carbons uretidione carbonyl carbons uretidione nitrogens
 <p align="center"><i>p</i>-tolyluretidione</p>	1 2 3 4 CH <sub>3</sub> CO N	134 <sup>i,j</sup> 117 130 132 21 151	145 <sup>j</sup> (145) <sup>l</sup>	nitrogen-substituted carbons unsubstituted ortho carbons unsubstituted meta carbons methyl-substituted para carbons methyl carbons uretidione carbonyl carbons uretidione nitrogens
 <p align="center">phenylisocyanurate</p>	1 2 3 4 CO N	134 <sup>m,n</sup> (133) <sup>o</sup> 128 (129) 129 (129) 129 (129) 149 (150)	149 <sup>n</sup>	nitrogen-substituted carbons unsubstituted ortho carbons unsubstituted meta carbons unsubstituted para carbons isocyanurate carbonyl carbons isocyanurate nitrogens
 <p align="center"><i>p</i>-tolylisocyanurate</p>	1 2 3 4 CH <sub>3</sub> CO N	134 <sup>m,n</sup> (133) <sup>p</sup> 130 (130) 130 (130) 139 (138) 21 (22) 150 (149)	149 <sup>n</sup> (149) <sup>q</sup>	nitrogen-substituted carbons unsubstituted ortho carbons unsubstituted meta carbons methyl-substituted para carbons methyl carbons isocyanurate carbonyl carbons isocyanurate nitrogens
 <p align="center">phenylurea</p>	1 2 3 4 CO N	140 <sup>r,s</sup> (139) <sup>t</sup> 118 129 (130) 122 153 (156)	106 <sup>s</sup> (106) <sup>u</sup>	nitrogen-substituted carbons unsubstituted ortho carbons unsubstituted meta carbons unsubstituted para carbons urea carbonyl carbons urea nitrogens
 <p align="center"><i>p</i>-tolylurea</p>	1 2 3 4 CH <sub>3</sub> CO N	137 <sup>r,s</sup> 118 129 131 20 153	107 <sup>s</sup>	nitrogen-substituted carbons unsubstituted ortho carbons unsubstituted meta carbons methyl-substituted para carbons methyl carbons urea carbonyl carbons urea nitrogens

Table I (Continued)

prototype structure	carbon or nitrogen	$^{13}\text{C}$ chem shift, ppm	$^{15}\text{N}$ chem shift, ppm	description <sup>b</sup>
 phenylbiuret	1	139 <sup>u,w</sup>		amide-substituted carbons
	2	122		unsubstituted ortho (to NH) carbons
	3	130		unsubstituted meta (to NH) carbons
	4	125		unsubstituted para (to NH) carbons
	1'	138		imide-substituted carbons
	2'	131		unsubstituted ortho (to N) carbons
	3'	131		unsubstituted meta (to N) carbons
	4'	130		unsubstituted para (to N) carbons
	CO	155		carbonyl carbons
	NH		116 <sup>w</sup>	amide nitrogens
	N		143	imide nitrogens
 p-tolylbiuret	1	140 <sup>u,w</sup> (141) <sup>x</sup>		amide-substituted carbons
	2	122 (120)		unsubstituted ortho (to NH) carbons
	3	130 (131)		unsubstituted meta (to NH) carbons
	4	134 (134)		methyl-substituted para (to NH) carbons
	CH <sub>3</sub>	21 (21)		para methyl (to NH) carbons
	1'	137 (136)		imide-substituted carbons
	2'	131 (132)		unsubstituted ortho (to N) carbons
	3'	131 (132)		unsubstituted meta (to N) carbons
	4'	135 (136)		methyl-substituted para (to N) carbons
	CH <sub>3</sub> '	20 (21)		para methyl (to N) carbons
	CO	155 (155)		carbonyl carbons
	NH		114 <sup>w</sup>	amide nitrogens
	N		143	imide nitrogens

<sup>a</sup> Parentheses indicate chemical shifts obtained from  $^{13}\text{C}$  and  $^{15}\text{N}$  CP/MAS or single-pulse MAS experiments. <sup>b</sup> Ortho, meta, and para designations are relative to the nitrogen-substituted carbon. <sup>c</sup> Delides, C.; Pethrick, R. A.; Cunliffe, A. V.; Klein, P. G. *Polymer* **1981**, *22*, 1205. <sup>d</sup> 37.5-MHz  $^{13}\text{C}$  single-pulse MAS experiment, repetition delay =  $t_d = 55$  s. <sup>e</sup> Sibi, M. P.; Lichter, R. L. *J. Org. Chem.* **1979**, *44*, 3017. <sup>f</sup> CP contact time =  $\tau = 6$  ms; repetition delay =  $t_d = 30$  s. <sup>g</sup> 1.5 g in 8 mL of dimethyl sulfoxide. <sup>h</sup>  $\tau = 1$  ms;  $t_d = 200$  s. <sup>i</sup> Prepared as in: Raiford, L. C.; Freyermuth, H. B. *J. Org. Chem.* **1943**, *8*, 230. <sup>j</sup> 0.5 g in 10 mL of benzene. <sup>k</sup>  $\tau = 3$  ms;  $t_d = 30$  s. <sup>l</sup>  $\tau = 6$  ms;  $t_d = 30$  s. <sup>m</sup> Prepared as in ref 4. <sup>n</sup> 1.0 g in 8 mL of acetone. <sup>o</sup>  $\tau = 3$  ms;  $t_d = 30$  s. <sup>p</sup>  $\tau = 3$  ms;  $t_d = 30$  s. <sup>q</sup>  $\tau = 6$  ms;  $t_d = 10$  s. <sup>r</sup> Prepared as in ref 36. <sup>s</sup> 1.0 g in 8 mL of dimethyl sulfoxide. <sup>t</sup>  $\tau = 3$  ms;  $t_d = 30$  s. <sup>u</sup>  $\tau = 1$  ms;  $t_d = 100$  s. <sup>v</sup> Prepared as in ref 40. <sup>w</sup> 0.5 g in 8 mL of acetone. <sup>x</sup> 37.5-MHz  $^{13}\text{C}$  CP/MAS experiment,  $\tau = 1.5$  ms;  $t_d = 10$  s.



**Figure 3.** 50.3-MHz  $^{13}\text{C}$  CP/MAS interrupted-decoupling spectra ( $\tau = 4$  ms, interrupt time = 70  $\mu\text{s}$ ) of the MDI-polyisocyanurate resins represented in Figure 2.

distinguished in the samples cured at 100 and 120 °C. Close examination of these five spectra reveals several distinct differences. Since the interrupted-decoupling experiment should dramatically reduce the signal at 125 ppm due to aromatic carbons ortho to an isocyanate substituent, the signal intensity remaining at 125 ppm should be primarily associated with the isocyanate carbonyl carbon. Qualitatively, the relative amount of unreacted isocyanate appears to be greatest for the cure temperatures of 100 and 160 °C, while the corresponding  $^{13}\text{C}$  intensity

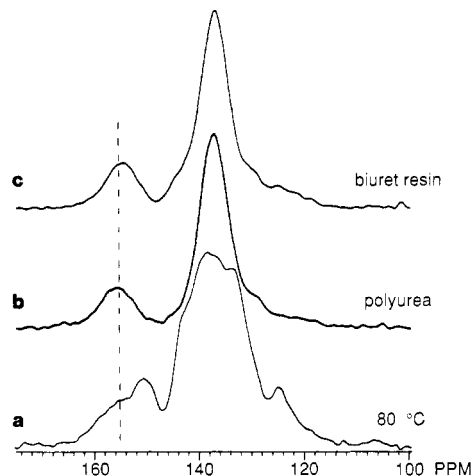


**Figure 4.** 50.3-MHz  $^{13}\text{C}$  CP/MAS interrupted-decoupling spectra ( $\tau = 4$  ms, interrupt time = 70  $\mu\text{s}$ ) of (a) MDI-polyisocyanurate cured at 80 °C, (b) the MDI-based polyurea, and (c) the MDI-based biuret resin. The dashed line indicates a spectral region discussed in the text.

is lowest at 120 °C. In addition, the relative intensity of the isocyanate carbonyl resonance (150 ppm) in Figure 3 appears to increase with increasing cure temperature up to 120 °C. At cure temperatures above 120 °C, the relative intensity of the isocyanate resonance decreases with increasing cure temperature. Qualitatively, it appears from the spectra shown in Figure 3 that isocyanate formation is most favored at ca. 120 °C under these particular reaction conditions.

Substantial spectral intensity exists in the spectral region corresponding to lower shielding than the isocyanate carbonyl resonance (150 ppm) for the MDI-polyisocyanurate resin cured at 80 °C (shown in Figure 3; see the arrow). Three different linkages can give rise to spec-

tral intensity in this region. Table I shows that the  $^{13}\text{C}$  chemical shift of the amide and imide carbonyl carbons of a MDI-biuret type network is 155 ppm, while the  $^{13}\text{C}$  chemical shift of MDI-based urea linkages is 156 ppm. The 50.3-MHz  $^{13}\text{C}$  CP/MAS interrupted-decoupling results for the MDI-polyisocyanurate resin cured at 80 °C, the MDI-based polyurea polymer,<sup>35</sup> and the MDI-based biuret resin<sup>36</sup> are shown in Figure 4. Both the interrupted-decoupling spectra of the MDI-based polyurea and the MDI-based biuret resin have spectral intensity centered about 155 and 137 ppm. When these spectra are compared to the interrupted-decoupling spectrum obtained for the MDI-polyisocyanurate resin cured at 80 °C, it becomes clear that distinguishing these various linkages on the basis of the  $^{13}\text{C}$  chemical shift alone is highly problematic. Schemes I-IV imply that all three linkages should be possible, depending on the reaction conditions. Although the  $^{13}\text{C}$  CP/MAS interrupted-decoupling results for the MDI-polyisocyanurate resin cured at 80 °C presented in Figures 3 and 4 indicate the presence of some other chemical species besides isocyanurate moieties and unreacted isocyanate, the unambiguous identification of this additional species is at this point impossible.

The relative intensity of the isocyanate carbonyl resonance (125 ppm) appears to be smaller for the MDI-polyisocyanurate cured at 80 °C compared with the MDI-polyisocyanurate cured at 100 °C in Figure 3. The formation of either biuret or urea linkages, indicated by the increased spectral intensity centered about 155 ppm for the sample cured at 80 °C, can occur according to Schemes II-IV. Thus, at the lowest cure temperature of 80 °C, the data presented here would suggest that the formation of biuret and/or urea linkages is competitive with isocyanurate formation and that the combination of these pathways results in an increased consumption of isocyanate, relative to the case of the MDI-polyisocyanurate cured at 100 °C, where the formation of biuret and/or urea linkages is not prevalent.

The resonance at 143 ppm, which appears as a shoulder in the spectra of Figure 3 for the samples cured at 80, 140, and 160 °C, is more clearly resolved in the spectra corresponding to the samples cured at 100 and 120 °C. Table I shows that methyl-substituted aromatic carbons para to an isocyanurate nitrogen have a chemical shift of 139 ppm. Additivity rules<sup>37,38</sup> can be invoked to predict a chemical shift of 142 ppm for a benzyl-substituted carbon positioned para to the isocyanurate nitrogen. Therefore, the resonance at 143 ppm corresponds to a benzyl-substituted aromatic carbon para to an isocyanurate nitrogen. Also, note from Figure 3 that the spectral intensity in the region centered at 138 ppm (benzyl-substituted aromatic carbon para to an isocyanate moiety) appears larger for the higher cure temperatures of 140 and 160 °C, while the relative amount of isocyanurate (150 ppm) is correspondingly smaller.

While the apparent increase in spectral intensity in the 137 ppm region for the MDI-polyisocyanurate cured at 80 °C can be rationalized by the substantial formation of amide, imide, and/or urea linkages (see Table I for nitrogen-substituted aromatic carbon chemical shifts), no such argument exists for the samples cured at 140 and 160 °C. Since little spectral intensity is seen at lower shielding than 150 ppm in the spectra of the samples prepared at these higher cure temperatures (Figures 2 and 3), it seems unlikely that a significant number of urea, amide, or imide linkages exists in these resin systems, as the carbonyl resonances of these linkages are expected to occur at ca. 155 ppm. However, Table I shows

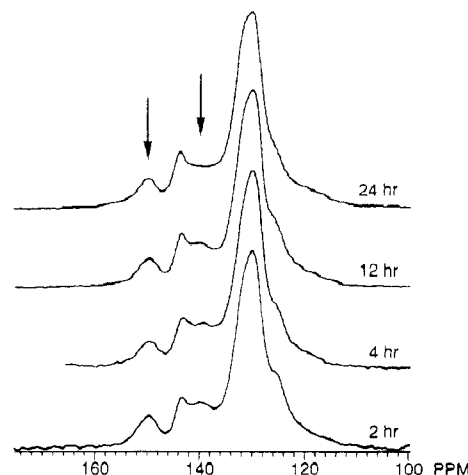


**Figure 5.** 50.3-MHz  $^{13}\text{C}$  CP/MAS spectra ( $\tau = 4$  ms) of MDI-polyisocyanurate resins prepared at 120 °C as a function of cure time.

that the resonance attributed to methylene-substituted carbons with para isocyanate functionalities is found at 138 ppm. Close examination of this spectral region in Figure 3 for the MDI-polyisocyanurate resins cured at 120, 140, and 160 °C shows a distinct increase in spectral intensity for this region as the cure temperature of these samples is increased. The intensity of the resonance of the unreacted isocyanate group itself (125 ppm) in Figure 3 also appears to increase as the cure temperature is increased for the samples cured at 120, 140, and 160 °C. Although isocyanurate formation is known to be favored at higher temperatures,<sup>22</sup> this data set would suggest that, under the reaction conditions specified, there exists an optimal curing temperature near 120 °C for isocyanurate formation; above this temperature, the net formation of isocyanurate moieties is diminished.

Since the decomposition temperature of the stannous octoate is known to be above 160 °C,<sup>39</sup> one can rule out catalyst decomposition as an explanation for the decreased isocyanurate formation at the higher cure temperatures. Also, from the increase in relative intensity of unreacted isocyanate carbons at higher cure temperatures, compared with lower cure temperatures, decomposition of the isocyanate itself can be ruled out as an explanation for decreased isocyanurate formation. However, it is possible that the catalytic activity of the stannous octoate is decreased at these higher temperatures.<sup>8</sup>

The extent to which isocyanurate formation could be enhanced by optimizing the cure time was investigated by increasing the cure time under conditions of "optimal" cure temperature. The 120 °C cure temperature was chosen for this purpose, because it appears to yield the highest relative amount of isocyanurate in Figures 2 and 3. Figure 5 shows the 50.3-MHz  $^{13}\text{C}$  CP/MAS spectra of four samples cured at 120 °C for different periods. Qualitatively, the only change in these spectra from the shortest to the longest cure time is the decrease in spectral intensity in the region between 138 and 140 ppm, which corresponds to benzyl-substituted aromatic carbons with isocyanate functionalities para to them. This decrease becomes more obvious in the interrupted-decoupling results shown in Figure 6. Clearly, intensity in the region between 138 and 140 ppm (see the middle arrow) is decreased as the cure time is increased. In addition, the relative intensities of the resonances at 150 ppm (left arrow) and 143 ppm are seen to increase with increasing cure time. The relative intensity of the unreacted isocyanate (right arrow) does not appear to vary signifi-

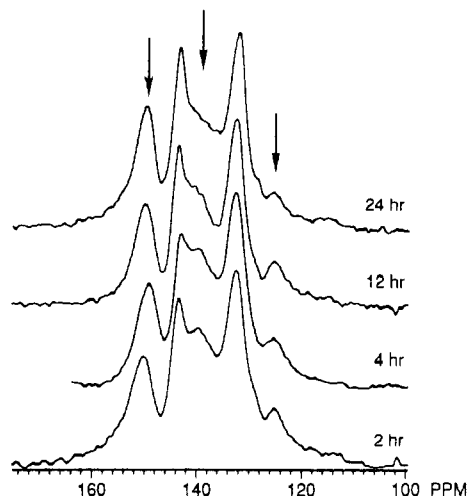


**Figure 6.** 50.3-MHz  $^{13}\text{C}$  CP/MAS interrupted-decoupling spectra ( $\tau = 4$  ms, interrupt time = 70  $\mu\text{s}$ ) of MDI-polyisocyanurate resins prepared at 120  $^{\circ}\text{C}$  as a function of cure time.

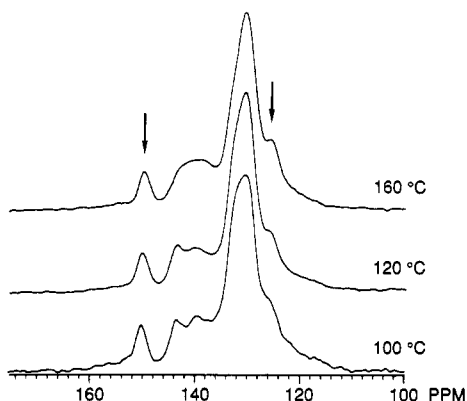


**Figure 7.** 50.3-MHz  $^{13}\text{C}$  CP/MAS spectra ( $\tau = 4$  ms) of three  $^{15}\text{N}$ -enriched MDI-polyisocyanurate resins prepared at different cure temperatures.

cantly, but does appear lowest for the sample cured for 24 h.

Although the  $^{13}\text{C}$  CP/MAS interrupted-decoupling spectra of the various MDI-polyisocyanurate systems reveal certain valuable qualitative patterns, a true estimate of the amount of isocyanurate formed or the amount of unreacted isocyanate remaining is made difficult because of two issues. These are (1) the largely qualitative nature of the interrupted-decoupling experiment and (2) the relatively complex nature of the  $^{13}\text{C}$  spectra, with overlapping resonances.

Three MDI-polyisocyanurate resins were prepared from  $^{15}\text{N}$ -enriched MDI (99.8% doubly labeled) at different cure temperatures. Figure 7 shows the most relevant region of the 50.3-MHz  $^{13}\text{C}$  CP/MAS results for samples cured at 100, 120, and 160  $^{\circ}\text{C}$ . Comparing these spectra with the  $^{13}\text{C}$  CP/MAS results in Figures 2 and 5 for MDI-polyisocyanurate resins prepared from MDI containing  $^{14}\text{N}$  (and  $^{15}\text{N}$ ) in natural abundance, one sees that some of the resonances (especially the isocyanurate carbonyl resonance at 150 ppm) are marginally more clearly resolved in the spectra of  $^{15}\text{N}$ -enriched samples. The  $^{13}\text{C}$  line widths of those  $^{13}\text{C}$  atoms directly attached to nitrogen might be expected to decrease upon isotopic substitution of  $^{14}\text{N}$  with  $^{15}\text{N}$ , since the quadrupolar/dipolar broadening influences due to  $^{14}\text{N}$  are removed.

Figure 8 shows the 50.3-MHz  $^{13}\text{C}$  CP/MAS interrupted-decoupling spectra of the  $^{15}\text{N}$ -enriched MDI-polyisocyanurate resins prepared at three temperatures. The relative peak areas in deconvolutions of these spec-

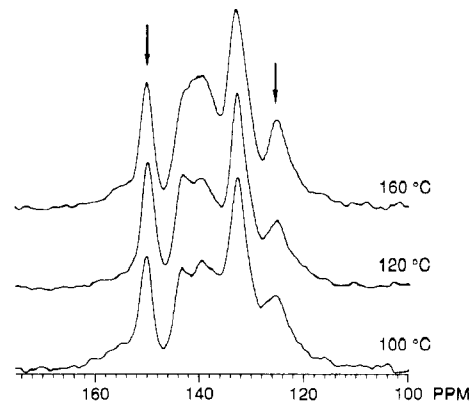


**Figure 8.** 50.3-MHz  $^{13}\text{C}$  CP/MAS interrupted-decoupling spectra ( $\tau = 4$  ms, interrupt time = 70  $\mu\text{s}$ ) of three  $^{15}\text{N}$ -enriched MDI-polyisocyanurate resins prepared at different cure temperatures.

tra indicate that the amount of isocyanurate (150 ppm) formed is largest for the sample cured at 120  $^{\circ}\text{C}$ , followed in order by the samples cured at 160 and 100  $^{\circ}\text{C}$ , respectively. Similarly, the resonance centered at 143 ppm, corresponding to benzyl-substituted aromatic carbons para to isocyanurate moieties, is largest for the 120  $^{\circ}\text{C}$  cure, followed by the 160  $^{\circ}\text{C}$  cure and the 100  $^{\circ}\text{C}$  cure, respectively. The amount of unreacted isocyanate (125 ppm) is largest, based on relative deconvoluted peak areas, for the sample cured at 160  $^{\circ}\text{C}$ , while the samples cured at 100 and 120  $^{\circ}\text{C}$  yield essentially identical relative peak areas for this resonance. Although trends corresponding to unreacted isocyanate were discernible in the  $^{13}\text{C}$  CP/MAS interrupted-decoupling results presented in Figure 3 and discussed above, no clear trend corresponding to unreacted isocyanate was observed for the data set represented in Figure 8. In any case, the results represented by Figures 3 and 8 cannot be readily compared because (1) the data set for the  $^{15}\text{N}$ -enriched MDI-polyisocyanurate resins was significantly smaller and (2) the MDI starting materials were not the same for the labeled and unlabeled cases. (The small quantity of the  $^{15}\text{N}$ -labeled MDI precluded its scrupulous purification.)

$^{15}\text{N}$  CP/MAS NMR might be expected to have various advantages over  $^{13}\text{C}$  CP/MAS for the study of polymer systems based on MDI.  $^{15}\text{N}$  has a larger chemical shift range than  $^{13}\text{C}$  for the likely structural possibilities in these systems and therefore a smaller likelihood of overlapping resonances. Also, there are fewer chemically distinct types of nitrogen moieties than carbon moieties in such systems, which should lead to simpler spectra and easier identification of peaks. Byproducts and/or minor products that would probably go undetected in the complicated  $^{13}\text{C}$  spectra may be detectable in the  $^{15}\text{N}$  spectra because of the first two advantages. Furthermore, well-resolved resonances lend themselves to quantitative treatment more readily. The main disadvantages of  $^{15}\text{N}$  CP/MAS NMR compared to  $^{13}\text{C}$  CP/MAS are (1) the lower natural abundance of  $^{15}\text{N}$  (0.37 vs 1.1% for  $^{13}\text{C}$ ) and (2)  $^{15}\text{N}$ 's lower inherent sensitivity based on the magnetogyric ratio,  $\gamma$ , which is only 40% that of  $^{13}\text{C}$ . Therefore, isotopic enrichment is usually required. Complete or nearly complete isotopic enrichment in  $^{15}\text{N}$  has the additional benefit, as indicated above, of improving resolution in the  $^{13}\text{C}$  CP/MAS spectra somewhat. The 20.3-MHz  $^{15}\text{N}$  CP/MAS spectra of the three  $^{15}\text{N}$ -enriched MDI-polyisocyanurate resins referred to above are shown in Figure 9 for three cure temperatures. The proposed structures in terms of which the  $^{15}\text{N}$  spectra are interpreted and tentative  $^{15}\text{N}$  peak assignments for

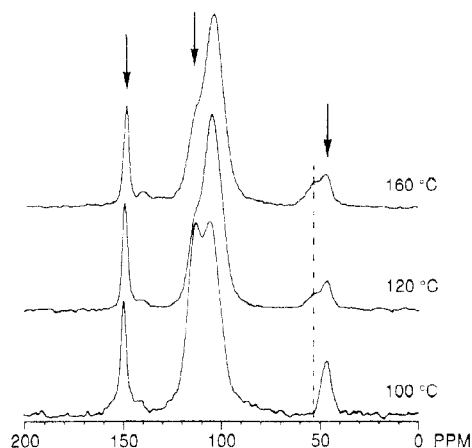


**Figure 9.** 20.3-MHz  $^{15}\text{N}$  CP/MAS spectra ( $\tau = 0.4$  ms) of three  $^{15}\text{N}$ -enriched MDI-polyisocyanurate resins prepared at different cure temperatures. The arrows and dashed line in the figure correspond to specific resonances or spectral regions discussed in the text.

those structures are shown in Table I.

The two peaks at 150 ppm (left arrow) and 46 ppm (right arrow) in each spectrum of Figure 9 correspond to the isocyanurate and isocyanate nitrogens, respectively. Since these spectra were obtained by using a relatively short contact time (0.4 ms), the experiment is not optimized for the observation of nitrogen nuclei with no directly attached hydrogens, e.g., isocyanurate and isocyanate nitrogens (vide infra). In addition to these two resonances, several other peaks are clearly visible in the spectra shown in Figure 9. On the basis of liquid-solution and solid-state  $^{15}\text{N}$  data (see Table I), we can see that the resonance centered at ca. 104 ppm corresponds to MDI-polyurea linkages. The partial hydrolysis of MDI to form urea linkages, as described in Scheme III, is well documented.<sup>22,40</sup> The 104 ppm resonance is also present in the 20.3-MHz  $^{15}\text{N}$  CP/MAS spectrum of the  $^{15}\text{N}$ -enriched MDI starting material (not shown here), indicating that the partial hydrolysis of MDI occurs quite readily with even minimal exposure to air.<sup>41</sup> This resonance is the dominant feature in the spectral region between 100 and 120 ppm in spectra of the MDI-polyisocyanurate resin samples cured at 120 and 160 °C, shown in Figure 9. A discernible shoulder at ca. 114 ppm (middle arrow) on the low-shielding side of the peak centered at 104 ppm clearly exists in the spectra of these two samples. This 114 ppm resonance, which is nearly equal in intensity to the 104 ppm resonance for the sample cured at 100 °C, is attributed on the basis of liquid-state data (see Table I) to an amide nitrogen in a biuret-type network. As shown in Scheme II, a termination step in the Lewis acid catalyzed isocyanate polymerization can lead to the formation of an amide linkage by reaction with trace amounts of water. Alternatively, biuret linkages can be formed from the reaction of isocyanate groups with urea linkages according to Scheme IV.

The increased intensity of the  $^{15}\text{N}$  resonance at 114 ppm for the sample cured at 100 °C, relative to the samples cured at 120 and 160 °C, is most probably the result of increased biuret branching. Since MDI is a difunctional monomer, the MDI chemistry is more complicated than what is shown explicitly in the reaction schemes above; branching from any available isocyanate group contained in R is possible, resulting in the formation of biuret linkages. Since the dominant formation of isocyanurate structures is favored at higher temperatures, the relative amounts of other available *branching* sites for samples cured at higher temperatures should be less than for sam-

ples cured at lower temperatures. Although the amount of biuret formation never approaches the amount of isocyanurate formation for any of the three  $^{15}\text{N}$ -enriched MDI-polyisocyanurate resins, it appears from this data set that biuret formation from Scheme II and/or Scheme IV is favored at 100 °C relative to 120 and 160 °C cure temperatures. Amide linkages (see biurets in Table I), as well as urea-type linkages, should dominate the spectra obtained with shorter CP contact times, i.e., under conditions that favor observation of nitrogen with directly attached hydrogen. Therefore, the broad spectral region between 100 and 120 ppm in the spectra of Figure 9 contains two distinct nitrogen environments, namely, the MDI-polyurea linkage at 104 ppm and the amide linkage of a biuret-type network at 114 ppm.

The small resonance at 141 ppm in each  $^{15}\text{N}$  CP/MAS spectrum of Figure 9 is not visibly attenuated in the interrupted-decoupling experiment (results discussed later) and therefore corresponds to a nitrogen moiety with no directly attached hydrogen(s). This peak can be attributed to an imide nitrogen (vide infra) in the biuret-type network, based on liquid-solution  $^{15}\text{N}$  data (see Table I).

The isocyanate resonances at 46 ppm in the  $^{15}\text{N}$  spectra of the samples cured at 120 and 160 °C in Figure 9 are complicated by the presence of a shoulder centered at 53 ppm. This region can be attributed to aromatic amine groups on the basis of liquid-solution and solid-state  $^{15}\text{N}$  data (see Table I). Surprisingly, the sample cured at 100 °C in Figure 9 does not show the presence of the amine moiety. Clearly, the most straightforward explanation for the formation of amine groups would be a reaction of free isocyanate with traces of water or other protic sources. Once the amine is formed, it quickly reacts with excess isocyanate to form urea linkages, as shown in Scheme III. Apparently, at least for the samples cured at 120 and 160 °C, the reactivity of available isocyanate groups allows for the significant formation of amine groups which, once formed, do not react with additional isocyanate to form urea linkages. The absence of unreacted amine groups in the sample cured at 100 °C might be associated with the observed maximum in biuret formation at that cure temperature. The stannous octoate catalyzed formation of isocyanurate cross-links is the dominant reaction for all temperatures examined in the  $^{15}\text{N}$ -enriched MDI-polyisocyanurate resin sample set. However, biuret formation is favored by lower temperatures, as indicated in Figure 9 by the increased spectral intensity observed at 114 ppm for the sample cured at 100 °C. Since, according to Schemes I and II, isocyanurate formation does not proceed with the consumption of water and biuret formation does, perhaps the reaction of water at the lower cure temperature to produce biuret linkages precludes the significant formation of the amine during the low-temperature curing process. Although the amine is easily identified in two of the spectra of Figure 9, it should be noted that its spectral intensity amounts to <3% of the total observed spectral intensity for each sample.

Figure 10 shows the  $^{15}\text{N}$  CP/MAS spectra of the three  $^{15}\text{N}$ -enriched MDI-polyisocyanurate resins obtained under cross-polarization conditions (6-ms contact time) that favor observation of the isocyanurate and isocyanate nitrogens. The two major peaks (see arrows) at 150 and 46 ppm in each  $^{15}\text{N}$  CP/MAS spectrum correspond to the isocyanurate and isocyanate nitrogens, respectively. From these spectra, it is readily apparent that the relative amount of unreacted isocyanate is least in the sample cured at 120 °C, followed by the sample cured at 160 °C, and is



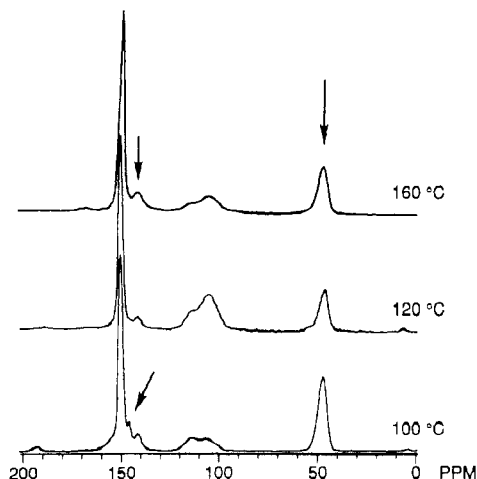


**Figure 10.** 20.3-MHz  $^{15}\text{N}$  CP/MAS spectra ( $\tau = 6$  ms) of three  $^{15}\text{N}$ -enriched MDI-polyisocyanurate resins prepared at different cure temperatures.

considerably larger in the sample cured at 100 °C. The unreacted isocyanate groups in these samples can a priori exist in the form of (a) unreacted MDI monomer or (b) "half-reacted" MDI, i.e., a system in which one of the original isocyanate groups of MDI remains intact and one has reacted to form either a monomeric species or an oligomeric or polymeric species. Solid-state  $^{15}\text{N}$  NMR methods for distinguishing between unreacted monomer and terminal isocyanate groups in these resins are currently being investigated and will be addressed in a subsequent publication. In addition to these two resonances, other peaks are clearly visible in the spectra shown in Figure 10. The resonances between 100 and 120 ppm, corresponding to the urea and amide linkages, are strongly attenuated under these experimental conditions because of cross-polarization dynamics (vide infra). The small resonance at 141 ppm in each  $^{15}\text{N}$  spectrum of Figure 10 (upper left arrow) corresponds to the imide linkage in the MDI-biuret type network, as indicated above for the spectra in Figure 9. This resonance is more distinct in Figure 10 relative to Figure 9, since the imide nitrogen, like the isocyanurate and isocyanate nitrogens, bears no directly attached hydrogen(s). Another resonance can be seen, at 145 ppm, in the spectrum of the sample cured at 100 °C in Figure 10. On the basis of liquid-solution and solid-state  $^{15}\text{N}$  data (see Table I), this resonance is attributed to the uretidione linkage, whose formation is known to be favored under certain conditions, including slightly elevated temperatures.<sup>22,40</sup> There is no evidence of the amine groups in the spectra of Figure 10. Since the nitrogen atom in the amine group bears two hydrogens and is much lower in concentration than the urea and amide linkages, it is not detectable under the experimental conditions represented by Figure 10.

$^{15}\text{N}$  CP/MAS interrupted-decoupling experiments were performed on each  $^{15}\text{N}$ -enriched MDI-polyisocyanurate resin to confirm that the isocyanurate, isocyanate, imide, and uretidione resonances were due to nitrogen environments not bearing directly attached hydrogens. These results are shown in Figure 11. As expected, intensity in only the spectral region corresponding to nitrogen species bearing directly attached hydrogens, i.e., urea and amide linkages between 100 and 120 ppm, is strongly attenuated.

When the  $^{15}\text{N}$  CP/MAS results of Figure 10 are compared with the  $^{13}\text{C}$  CP/MAS interrupted-decoupling results in Figure 8, which were obtained on the same  $^{15}\text{N}$ -enriched MDI-polyisocyanurate samples, it appears that analyzing the  $^{15}\text{N}$  data for quantitative information should

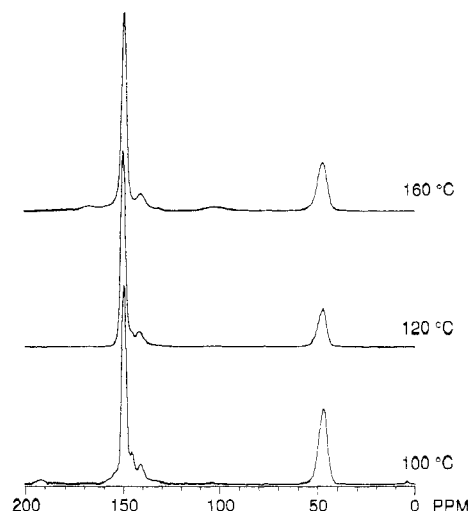


**Figure 11.** 20.3-MHz  $^{15}\text{N}$  CP/MAS interrupted-decoupling spectra ( $\tau = 6$  ms, interrupt time = 70  $\mu\text{s}$ ) of three  $^{15}\text{N}$ -enriched MDI-polyisocyanurate resins prepared at different cure temperatures.

be more straightforward than for the  $^{13}\text{C}$  case. To that end, variable contact time and  $^1\text{H}$  relaxation experiments were carried out to provide the information necessary for quantitation. Table II contains the results of the detailed set of relaxation experiments performed for each  $^{15}\text{N}$ -enriched MDI-polyisocyanurate resin. This table gives values obtained for the following three relaxation parameters for the three main peaks in the  $^{15}\text{N}$  CP/MAS spectra of Figure 10, namely, the isocyanurate resonance at 150 ppm, the polyurea resonance centered at ca. 104 ppm, and the isocyanate resonance at 46 ppm: (1)  $T_{1\text{H}}$ , the proton spin-lattice relaxation time; (2)  $T_{\text{NH}}$ , the cross-polarization relaxation time; and (3)  $T_{1\rho\text{H}}$ , the proton spin-lattice relaxation time in the rotating frame. The quantitative significance of the relative intensities of a CP/MAS spectrum can be evaluated by careful determination of these three parameters.

The results summarized in Table II show relatively large differences between the  $T_{1\rho\text{H}}$  values obtained for the 46 and 150 ppm resonances, compared to the values obtained for the 104 ppm resonance. The  $T_{1\rho\text{H}}$  value of a homogeneous solid is typically expected to be an average over all the protons in the sample, because of proton spin diffusion.<sup>42,43</sup> However, different  $T_{1\rho\text{H}}$  values have been observed in heterogeneous polymer systems containing distinct domains of differing molecular mobilities throughout the sample,<sup>44</sup> e.g., in samples containing both crystalline and amorphous regions.<sup>44-46</sup> Perhaps the polyurea environments (104 ppm), manifesting  $T_{1\rho\text{H}}$  values that are shorter by a factor of ca. 2.5-3.5 than  $T_{1\rho\text{H}}$  measured via isocyanate (46 ppm) and isocyanurate (150 ppm) nitrogens, undergo more efficient relaxation because of increased molecular motion relative to the isocyanate and isocyanurate environments. In the limit of large domain sizes, this kind of explanation can correspond to a classical phase separation between an isocyanurate/isocyanate-rich resin and a polyurea-rich resin.

A repetition time of 6 s was chosen for all the  $^{13}\text{C}$  and  $^{15}\text{N}$  CP/MAS experiments represented in the figures to ensure complete proton spin-lattice relaxation. Six seconds is more than 4 times the largest  $T_{1\text{H}}$  value displayed in Table II.

$^1\text{H}$ - $^{15}\text{N}$  cross-polarization transfer, represented by the rate constant  $T_{\text{NH}}^{-1}$ , and rotating-frame proton spin-lattice relaxation, represented by the rate constant  $T_{1\rho\text{H}}^{-1}$ , are competing effects, which determine the fraction of the theoretical CP intensity that is observed for each peak.

Table II  
<sup>15</sup>N Relaxation Parameters and Relative Intensities for <sup>15</sup>N-Enriched MDI-Polyisocyanurate Resins

sample cure <i>T</i> , °C	resonance, ppm	<i>T</i> <sub>1H</sub> , s	<i>T</i> <sub>NH</sub> , ms	<i>T</i> <sub>1ρH</sub> , ms	<i>M</i> ( <i>τ</i> = 6 ms)	<i>M</i> *	$\frac{M(\tau = 6 \text{ ms})}{M^*} \times 100$	$\frac{\text{isocyanurate}^a}{\text{isocyanate}}$
100 °C	150	1.1	3.0	17.4	48.8	70.6	69	1.6
	104	1.1	0.2	5.0	16.6	52.6	32	
	46	1.1	3.3	16.9	28.7	43.0	67	
120 °C	150	1.2	2.8	15.2	50.5	74.2	68	2.8
	104	1.2	0.1	4.5	26.2	94.7	27	
	46	1.2	3.2	13.7	16.7	26.2	64	
160 °C	150	1.1	2.5	10.3	48.8	79.3	62	2.3
	104	1.1	0.1	4.3	20.3	78.2	26	
	46	1.1	2.5	11.7	22.3	33.6	64	

<sup>a</sup> This mole ratio was calculated from intensities, using correction factors based on the preceding column.

A useful form of this relationship is given in eq 1.<sup>47</sup> In

$$M(\tau) = M^* \frac{T_{1\rho H}}{T_{1\rho H} - T_{CP}} (e^{-\tau/T_{1\rho H}} - e^{-\tau/T_{CP}}) \quad (1)$$

this equation *M*(*τ*) is the nitrogen magnetization observed for a given CP contact time, *τ*; and *M*\* is the nitrogen magnetization one would obtain if cross polarization were instantaneous and rotating-frame relaxation were infinitely slow. *T*<sub>CP</sub> = *T*<sub>NH</sub> for a <sup>15</sup>N CP experiment. Values of *T*<sub>NH</sub> and *T*<sub>1ρH</sub> were obtained by fitting the variable-contact data for eq 1 via a least-squares routine. Variations in *T*<sub>NH</sub> and *T*<sub>1ρH</sub> shown in Table II, especially comparing the isocyanurate and isocyanate values with those obtained for the polyurea, would make quantitative analysis of the data for a given contact time impossible, if the *T*<sub>NH</sub> and *T*<sub>1ρH</sub> values had not been determined. However, knowing the *T*<sub>NH</sub> and *T*<sub>1ρH</sub> values from the variable contact time experiment, one can correct the intensities according to eq 1 for a given contact time to obtain the corresponding corrected CP-enhanced magnetizations.

The magnetization observed for *τ* = 6 ms, *M*(*τ* = 6 ms), and the corrected magnetization, *M*\*, are included (in arbitrary units) in Table II for the isocyanurate and isocyanate resonance for each <sup>15</sup>N-enriched MDI-polyisocyanurate. In addition, the percentage of the theoretical maximum intensity observed and the correspondingly corrected ratio of isocyanurate intensity to isocyanate intensity are given. From these data, it is apparent that, although the observed intensity for each resonance is significantly lower than the theoretical maximum, the extent of cross-polarization efficiency is nearly the same for the two resonances of interest.

Although the relative intensities of the standard and interrupted-decoupling <sup>13</sup>C CP/MAS spectra in Figures 7 and 8 indicate that isocyanurate formation is most favored at 120 °C, that type of data does not lend itself to quantitative treatment. The <sup>15</sup>N CP/MAS data not only agree qualitatively with the <sup>13</sup>C CP/MAS data but provide a much more detailed interpretation of the curing behavior in these MDI-polyisocyanurate resin systems. The results of Table II clearly show that the formation of isocyanurate cross-links is favored most at 120 °C, among the temperatures examined, followed by 160 and 100 °C, respectively. The amount of unreacted isocyanate was considerably larger (ca. 38%) for the lowest cure temperature of 100 °C than for the highest cure temperature of 160 °C (30%), a result that would be impossible to ascertain from only the <sup>13</sup>C data presented in Figures 7 and 8. Although isocyanurate formation is known to be favored by higher temperatures, clearly an optimal temperature is indicated from the <sup>15</sup>N CP/MAS data (ca. 120 °C for this data set), above which isocyanurate for-

mation decreases. These quantitative data also agree with the qualitative <sup>13</sup>C CP/MAS and <sup>13</sup>C CP/MAS interrupted-decoupling results obtained on MDI-polyisocyanurate resins containing <sup>14</sup>N in natural abundance and represented by the spectra in Figures 2 and 3. However, the <sup>15</sup>N CP/MAS results summarized in Table II allow a numerical estimate for the decrease in isocyanurate formation in progressing from 120 to 160 °C. The straightforward analysis of these complex, insoluble resins to yield detailed information on the curing behavior is made possible by the ability of <sup>15</sup>N CP/MAS NMR to resolve the isocyanurate and isocyanate resonances.

### Summary and Conclusions

<sup>13</sup>C CP/MAS NMR monitoring of the curing of MDI-polyisocyanurate resin systems has established an optimal curing temperature of ca. 120 °C, under the conditions specified, by measurement of the relative amounts of isocyanurate formed and unreacted isocyanate present. The amount of isocyanurate formed was also found to increase upon increasing the curing time at 120 °C. Close examination of spectra obtained for various cure temperatures showed significant differences, establishing the fact that some other chemical species are formed in the MDI-polyisocyanurate resin cured at 80 °C. However, even with the aid of spectra from an MDI-polyurea and an MDI-based biuret resin system, unambiguous identification of such species could not be accomplished by <sup>13</sup>C CP/MAS NMR, because the spectra of MDI-polyisocyanurate resins are quite complex, with overlapping resonances. The inability of <sup>13</sup>C CP/MAS NMR to distinguish these particular environments makes the identification of the pathways competing with isocyanurate formation impossible by <sup>13</sup>C CP/MAS NMR alone at this stage of the state-of-the-art. This situation renders identification of some species difficult and virtually precludes the identification of minor products or a straightforward quantitative analysis by <sup>13</sup>C CP/MAS alone. Hence, the utility of <sup>13</sup>C CP/MAS NMR in the MDI-resin context is largely qualitative.

The <sup>15</sup>N CP/MAS results yielded simpler spectra than their <sup>13</sup>C CP/MAS counterparts and minor products in the spectra were clearly identified. The fate of the reactive isocyanate functionality was readily monitored, resulting in the unambiguous spectral identification of the following linkages or functionalities: the isocyanurate linkage at 150 ppm, the uretidione linkage at 145 ppm, the imide linkage at 141 ppm, the amide linkage at 114 ppm, the urea linkage at 104 ppm, the amine at 53 ppm, and unreacted isocyanate at 46 ppm. In comparison, <sup>13</sup>C CP/MAS was able to identify clearly just the isocyanurate linkage at 150 ppm and the unreacted isocyanate at 125 ppm. In addition, when the appropriate cross-polarization dynamics were considered, quantitative <sup>15</sup>N

CP/MAS results were obtained. The  $^{15}\text{N}$  CP/MAS results confirmed the fact, established by  $^{13}\text{C}$  data, that the extent of cross-linking via isocyanurate ring formation was greatest at 120 °C. The enhanced structural information content of the  $^{15}\text{N}$  CP/MAS results clearly demonstrates the advantage of using this technique (currently with  $^{15}\text{N}$  enrichment) over  $^{13}\text{C}$  CP/MAS as a solid-state NMR technique for these particular types of chemical systems at the present time. Since nitrogen-containing moieties will be involved with most, if not all, of the formation chemistry of isocyanate-based resin systems,  $^{15}\text{N}$  CP/MAS NMR will be a powerful technique for probing the relevant structures.

**Acknowledgment.** We gratefully acknowledge support of this research by NSF Grant No. DMR-85-4818846, the use of the Colorado State University Regional NMR Center funded by National Science Foundation Grant CHE-8616437, and helpful discussions with Dr. I-Ssuer Chuang.

## References and Notes

- Schollenberger, C. S. *Handbook of Adhesives*; Skeist, I., Ed.; Van Nostrand Reinhold: New York, 1977.
- Urethane Chemistry and Applications*; Edwards, K. N., Ed.; American Chemical Society: Washington, DC, 1981.
- Urethane Science and Technology*; Frisch, K. C., Reegen, S. L., Eds.; Technomic Publishing Co.: Westport, CT, 1973; Vol. 2.
- Sandler, S. R. *J. Appl. Polym. Sci.* **1967**, *11*, 811.
- Frisch, K. C.; Patel, K. J.; Marsh, R. D. *J. Cell. Plast.* **1970**, *6*, 203.
- Reymore, H. E., Jr.; Carleton, P. S.; Kolakowski, R. A.; Sayigh, A. A. R. *J. Cell. Plast.* **1975**, *11*, 328.
- Wang, C. L.; Klempner, D.; Frisch, K. C. *J. Appl. Polym. Sci.* **1985**, *30*, 4337.
- Imai, Y.; Hidai, T.; Inukai, T.; Nakanishi, T. *Cell. Polym.* **1986**, *5*, 13.
- Imai, Y.; Hidai, T.; Inukai, T.; Nakanishi, T. *Cell. Polym.* **1986**, *5*, 25.
- Barikani, M.; Hepburn, C. *Cell. Polym.* **1986**, *5*, 169.
- Zamek, O. S.; Stein, R. J. U.S. Patent 4,607,103, 1986.
- Kuhn, E.; Den Boer, J.; Thoen, J. U.S. Patent 4,607,064, 1986.
- Pines, A.; Gibby, M. G.; Waugh, J. S. *J. Chem. Phys.* **1973**, *59*, 569.
- Schaefer, J.; Stejskal, E. O. *J. Am. Chem. Soc.* **1976**, *98*, 1031.
- Schaefer, J.; Stejskal, E. O. *Topics in Carbon-13 NMR Spectroscopy*; Levy, G. C., Ed.; Wiley: New York, 1979; Vol. 1.
- Fyfe, C. A.; Rudin, A.; Tchir, W. *J. Macromolecules* **1980**, *13*, 1322.
- Bryson, R. L.; Hatfield, G. R.; Early, T. A.; Palmer, A. R.; Maciel, G. E. *Macromolecules* **1983**, *16*, 1669.
- Fyfe, C. A.; McKinnon, M. S.; Rudin, A.; Tchir, W. *J. Macromolecules* **1983**, *16*, 1216.
- Maciel, G. E.; Chuang, I.-S.; Gollob, L. *Macromolecules* **1984**, *17*, 1081.
- Hatfield, G. R.; Maciel, G. E. *Macromolecules* **1987**, *20*, 608.
- Sebenik, A.; Osredkar, U.; Vizovisek, I. *J. Macromol. Sci., Chem.* **1986**, *A23*(3), 369.
- Frisch, K. C.; Rumao, L. P. *J. Macromol. Sci.—Rev. Macromol. Chem.* **1970**, *C5*(1), 103.
- Shashoua, V. E. *J. Am. Chem. Soc.* **1959**, *81*, 3156.
- Britain, J. W.; Gemeinhardt, P. G. *J. Appl. Polym. Sci.* **1960**, *4*, 207.
- Bartuska, V. J.; Maciel, G. E. *J. Magn. Reson.* **1981**, *42*, 312.
- Frye, J. S.; Maciel, G. E. *J. Magn. Reson.* **1982**, *48*, 125.
- Zhang, M.; Maciel, G. E. *J. Magn. Reson.* **1989**, *85*, 156.
- Alla, M.; Kundla, E.; Lippmaa, E. *JETP Lett.* **1978**, *27*, 208.
- Opella, S. J.; Frey, M. H.; Cross, T. A. *J. Am. Chem. Soc.* **1979**, *101*, 5856.
- Groombridge, C. J.; Harris, R. K.; Packer, K. J.; Say, B. J.; Tanner, S. F. *J. Chem. Soc., Chem. Commun.* **1980**, 474.
- Dixon, W. T. *J. Magn. Reson.* **1981**, *44*, 220.
- Wind, R. A.; Dec, S. F.; Lock, H.; Maciel, G. E. *J. Magn. Reson.* **1988**, *79*(1), 136.
- Delides, C.; Petrick, R. A.; Cunliffe, A. V.; Klein, P. G. *Polymer* **1981**, *22*, 1205.
- Opella, S. J.; Frey, M. H. *J. Am. Chem. Soc.* **1979**, *101*, 5854.
- The MDI-based polyurea or poly[methylenebis(4-phenylurea)] was prepared by the procedure given in: Sorenson, W. R. *J. Org. Chem.* **1959**, *24*, 978.
- The MDI-based biuret resin was prepared by the procedure given in: Ranney, M. W. *Isocyanates Manufacture*, Chemical Process Review No. 63, Noyes Data Corp., 1972, p 217.
- Grant, D. M.; Paul, E. G. *J. Am. Chem. Soc.* **1964**, *86*, 2984.
- Ewing, D. F. *Org. Magn. Reson.* **1979**, *12*, 499.
- Furusaki, T.; Kodaira, K.; Yamamoto, M.; Shimada, S.; Matsushita, T. *Mater. Res. Bull.* **1986**, *21*, 803.
- Arnold, R. G.; Nelson, J. A.; Verbanc, J. J. *J. Chem. Rev.* **1957**, *57*, 47.
- The 20.3-MHz  $^{15}\text{N}$  CP/MAS spectrum of the  $^{15}\text{N}$ -enriched MDI starting material contained a major resonance at 46 ppm corresponding to the isocyanate and a minor peak at 104 ppm corresponding to the urea linkage. This sample was not protected from air.
- Schaefer, J.; Stejskal, E. O.; Buchdahl, R. *Macromolecules* **1977**, *10*, 384.
- McCall, D. W. *Acc. Chem. Res.* **1971**, *4*, 223.
- Vanderhart, D. L.; Garroway, A. N. *J. Chem. Phys.* **1979**, *71*, 2773.
- McBrierty, V. J.; Douglass, D. C.; Falcone, D. R. *J. Chem. Soc., Faraday Trans. 2* **1972**, *68*, 1051.
- Havens, J. R.; Koenig, J. L. *Appl. Spectrosc.* **1983**, *37*, 226.
- Mehring, M. *High Resolution NMR Spectroscopy in Solids*, 2nd ed.; Springer-Verlag: Berlin, 1983; p 153.

**Registry No.** MDI (homopolymer), 25686-28-6; MDI, 101-68-8; MDA, 101-77-9; stannous octoate, 1912-83-0; phenyluretidione, 1025-36-1; *p*-tolyluretidione, 7342-77-0; phenyl isocyanurate, 1785-02-0; *p*-tolyl isocyanurate, 1785-03-1; phenylurea, 102-07-8; *p*-tolylurea, 621-00-1; phenylbiuret, 2645-39-8; *p*-tolylbiuret, 57148-24-0.